

Adaptive Docking Using Range Measurements

Barış Fidan, Soura Dasgupta. and Brian D. O. Anderson

Abstract—This paper presents an adaptive scheme for localization of a target from distance measurements and motion control of a mobile agent to pursue this target. First, a robust adaptive law is designed to generate location estimate of the target using distance measurements. Then, following the standard certainty equivalence approach, a motion control law is developed considering substitution of the estimate generated by the localization algorithm for the unknown location of the target. Noting that there is some incompatibility between the persistence of excitation requirements of the localization algorithm and the target pursuit goal of the motion control law, the base motion control law is designed to eliminate the effects of this incompatibility. Stability and convergence analysis for the overall adaptive control scheme is presented. The results are valid in both two and three dimensions of motion space.

I. INTRODUCTION

This paper deals with a simultaneous localization and motion control problem, bringing together two research fields which recently have gained significant interest: (*cooperative target localization* [2]-[6] and *target pursuit* [7]-[10]). Here, *localization* refers to the process of estimating the precise location of a target by sensory agent(s) using information related to the relative position to the target, whereas the target can be another sensory agent cooperating with the pursuing sensory agent(s) or a separate entity to be captured. We focus on docking of a single mobile agent A to a single target T .

For this task, A needs measurements providing information about the relative position of the target. These measurements can be in different forms, including range, bearing, power level (indirectly related to distance) and time difference of arrival (TDOA) measurements [2], [4], [11], [12]. Although the general problem of interest for this paper could be studied in parallel approaches for different forms of such measurements, we will focus on the range measurement case only. In abstract terms the problem of interest is the following:

Problem 1.1: Given an agent A with position $y : \mathbb{R} \rightarrow \mathbb{R}^n$ as a function of time t , and a target T located at an

An extended version of this paper [1] is accepted to appear in a special issue of the International Journal of Adaptive Control and Signal Processing.

B. Fidan is with Department of Mechanical and Mechatronics Engineering, University of Waterloo, Canada fidan@uwaterloo.ca

S. Dasgupta is with Department of Electrical and Electronics Engineering, University of Iowa, USA, soura-dasgupta@uiowa.edu. He was supported in part by US NSF grants CCF-0830747 and EPS-1101284 and a grant from the Roy J. Carver Charitable Trust

B.D.O. Anderson is Research School of Information Sciences and Engineering, Australian National University, Australia. Brian.Anderson@anu.edu.au. He was supported by the Australian Research Council under DP-110100538 and by National ICT Australia- NICTA. NICTA is funded by the Australian Government as represented by the Department of Broadband, Communications and the Digital Economy and the Australian Research Council through the ICT Center of Excellence program.

unknown position $x \in \mathbb{R}^n$, $n \in \{2, 3\}$, devise a control law that uniformly achieves:

$$\lim_{t \rightarrow \infty} \|y(t) - x\| = 0, \quad (\text{I.1})$$

using only the distance measurement,

$$D(t) = \|y(t) - x\| \quad (\text{I.2})$$

and the agent's own position $y(t)$.

In design of our adaptive localization and motion control scheme, we initially assume that the target T is stationary and the distance measurements are perfect; however we subsequently consider possible effects of drifts in the position of T in our adaptive law design, and analyze the effects of such drifts as well as measurement noises.

We approach Problem 1.1 using a parameter identifier based adaptive control framework [13], [14], where the localization of the target T by the mobile agent A is formulated as a parameter identification problem and a localization algorithm, in the form of a gradient adaptive law, is designed to produce the location estimates of T . The motion control of A is achieved using an adaptive controller based on the produced location estimates. The motion control law design is designed in a way to move the mobile agent towards \hat{x} , the location estimate generated by the localization algorithm.

The *localization algorithm*, described in Section II, permits the agent A to estimate the position x of T from measurements over an interval of $D(t)$, and is identical to a corresponding algorithm in [6], [7]. The novelty of this paper is in the *adaptive control design* described in Section III, noting that there is a *persistence of excitation* incompatibility between the localization and motion control tasks, and hence the adaptive control design here is not a trivial one.

The paper also provides stability and convergence analysis of the proposed adaptive control scheme in Section IV and a set of simulation results demonstrating the performance of the adaptive control scheme in Section VI. Concluding remarks are given in Section VII.

II. LOCALIZATION

In this section we focus on the localization (parameter identification) part of the adaptive control approach to Problem 1.1. The corresponding localization problem can be stated as follows:

Problem 2.1: Given an agent A with position $y : \mathbb{R} \rightarrow \mathbb{R}^n$ as a function of time t , and a target T located at an unknown position $x \in \mathbb{R}^n$, $n \in \{2, 3\}$, devise an adaptive law to generate the estimate $\hat{x}(t)$ of x such that

$$\lim_{t \rightarrow \infty} \|\hat{x}(t) - x\| = 0, \quad (\text{II.1})$$

using only the distance measurement,

$$D(t) = \|y(t) - x\| \quad (\text{II.2})$$

and the agent's own position $y(t)$.

A gradient-type localization algorithm has already been designed in [6] to solve Problem 2.1. To place the localization algorithm of [6] in the context of this paper, we note that [6] starts with the observation that because of (II.2), one obtains

$$\begin{aligned} \frac{d}{dt}D^2(t) &= 2\dot{y}^\top(t)(y(t) - x) \\ &= \frac{d}{dt}\|y(t)\|^2 - 2\dot{y}^\top(t)x, \end{aligned}$$

which, using the parameter identification framework of [13], [14], can be written in the linear parametric form

$$\bar{z}(t) = x^\top \bar{\phi}(t) \quad (\text{II.3})$$

where

$$\bar{z} = \frac{1}{2} \frac{d}{dt} (\|y(t)\|^2 - D^2), \quad \bar{\phi} = \dot{y}.$$

Note here that, as in [6], the unknown position vector x is assumed to be constant. Nevertheless, the effect of drifts in x have been analyzed in [6], and similarly, the effects of such drifts to Problem 1.1 will be discussed later in this paper.

Based on the parametric model (II.3), we propose the following *base* gradient algorithm to generate the estimate \hat{x} of x :

$$\begin{aligned} \dot{\hat{x}}(t) &= \gamma (\bar{z}(t) - \hat{z}(t)) \bar{\phi}(t), \\ \hat{z}(t) &= \hat{x}^\top(t) \bar{\phi}(t) \end{aligned} \quad (\text{II.4})$$

It is well known that in (II.4), $\hat{x}(t)$ converges exponentially to x , provided $\bar{\phi} = \dot{y}$ is *persistently exciting*, (*p.e.*), [13], [14], [15], with *p.e.* defined as follows:

Definition 2.1: [13], [14], [15] Consider any positive integer n and a signal $r : \mathbb{R} \rightarrow \mathbb{R}^n$. Then r is *p.e.* if there exist positive α_i and T_1 , such that for all t , there holds:

$$\alpha_1 I \leq \int_t^{t+T_1} r(\tau)r(\tau)^\top d\tau \leq \alpha_2 I$$

Essentially this requires that r persistently spans \mathbb{R}^n . The upper bound is simply a boundedness assumption. The α_i and T_1 will be called *p.e.* parameters. As shown in [6] for $n = 2$, \dot{y} being *p.e.*, is equivalent to the requirement that over every time interval of length T_1 , the minimum distance of $y(\cdot)$ from any straight line be larger than a number that grows with α_1 , i.e. y persistently avoids a linear trajectory. Similarly, for $n = 3$, y must persistently avoid a planar trajectory. This accords with intuition as in \mathbb{R}^2 , one must have distances from noncollinear points to achieve localization, just as in \mathbb{R}^3 one must have distances from noncoplanar points. Persistent avoidance of lines/planes stems from the need for exponential convergence.

Thus, (II.4) can serve as a localization step. *However its implementation requires generating the derivative of $D(t)$*

rendering it impractical. Instead, similarly to [6], we generate filtered versions of \bar{z} and $\bar{\phi}$ using the set of equations set out below:

$$z(t) = \dot{\zeta}_1(t) = -\alpha\zeta_1(t) + \frac{1}{2} (y^\top(t)y(t) - D^2(t)), \quad (\text{II.5})$$

$$\phi(t) = \dot{\zeta}_2(t) = -\alpha\zeta_2(t) + y(t), \quad (\text{II.6})$$

where $\alpha > 0$, $\zeta_1(0)$ is an arbitrary scalar and $\zeta_2(0)$ is an arbitrary vector. Correspondingly, the revised parametric model and localization become, respectively,

$$z(\cdot) \equiv x^\top \phi(\cdot) \quad (\text{II.7})$$

and

$$\begin{aligned} \dot{\hat{x}}(t) &= \gamma (z(t) - \hat{z}(t)) \phi(t), \\ \hat{z}(t) &= \hat{x}^\top(t) \phi(t), \end{aligned} \quad (\text{II.8})$$

where for two functions f_1, f_2 we say $f_1(\cdot) \equiv f_2(\cdot)$ if there exist $\lambda, M > 0$ such that for all $t \geq 0$, $\|f_1(t) - f_2(t)\| \leq Me^{-\lambda t}$; $\gamma > 0$ is the adaptive gain and $\hat{x}(0)$ is the initial estimate.

Although the derivation of the parametric model (II.7) is a standard modeling procedure [13], [14], the formal derivation in our case follows immediately from the following lemma:

Lemma 2.1: Consider (II.2),(II.5),(II.6) and assume that x is constant. Define

$$p(t) = x^\top \phi(t) - z(t) \quad (\text{II.9})$$

and

$$\tilde{x}(t) = \hat{x}(t) - x. \quad (\text{II.10})$$

Then there holds

$$\dot{p}(t) = -\alpha p(t) \quad (\text{II.11})$$

and

$$\dot{\tilde{x}}(t) = -\gamma \phi(t) \phi^\top(t) \tilde{x}(t) - \gamma \phi(t) p(t). \quad (\text{II.12})$$

Furthermore \tilde{x} converges to zero exponentially if ϕ is *p.e.*

Proof: Taking derivatives of both sides of (II.5) and (II.6), we obtain

$$\dot{z}(t) = -\alpha z + \bar{z}(t) \quad (\text{II.13})$$

$$\dot{\phi}(t) = -\alpha \phi(t) + \bar{\phi}(t) = -\alpha \phi(t) + \dot{y}(t) \quad (\text{II.14})$$

Substituting in (II.3) leads to (II.11). Taking derivatives of both sides of (II.10) and substituting (II.8),(II.9), we obtain (II.12).

Equation (II.11) implies that $p(t) \rightarrow 0$ exponentially as $t \rightarrow \infty$. This together with Definition 2.1 implies that, if ϕ is *p.e.*, then the state \tilde{x} of the linear time varying system II.12 converges to zero exponentially. ■

According to Lemma 2.1, exponential convergence of \hat{x} to x is obtained as long as ϕ is *p.e.*. This in turn requires that \dot{y} is *p.e.*. As will be evident in the sequel the control objective of Problem 1.1 is incompatible with a *p.e.* \dot{y} . The control law in the next section is partly motivated by this incompatibility.

III. THE CONTROL LAW

We suggest the motion control law to be in the form

$$\dot{y}(t) = \dot{\hat{x}}(t) - \beta(y(t) - \hat{x}(t)) + f(D(t))\dot{\sigma}(t), \quad (\text{III.1})$$

$$\dot{\sigma}(t) = A(t)\sigma(t), \quad (\text{III.2})$$

where $\beta > 0$ is a design constant, and $f : \mathbb{R}^+ \rightarrow \mathbb{R}^+$ (\mathbb{R}^+ standing for $[0, \infty)$) and $A(\cdot) : \mathbb{R} \rightarrow \mathbb{R}^{n \times n}$ are to be selected such that they obey the following assumptions.

Assumption 3.1: The function $f : \mathbb{R}^+ \rightarrow \mathbb{R}^+$ is a strictly increasing, differentiable, bounded function that is zero at zero, and satisfies $f(D) \leq D$, $\forall D \in \mathbb{R}^+$.

Assumption 3.2: (i) There exists a $T > 0$ such that for all t ,

$$A(t+T) = A(t), \quad (\text{III.3})$$

and $A(t)$ is bounded.

- (ii) $A(t)$ is skew symmetric for all t .
- (iii) $A(t)$ is differentiable everywhere.
- (iv) The derivative of σ in (III.2) is p.e. for any arbitrary nonzero value of $\sigma(0)$. More precisely, there exist positive $T_1, \alpha_i > 0$ such that for all $t \geq 0$ there holds

$$\alpha_1 \|\sigma(0)\|^2 I \leq \int_t^{t+T_1} \dot{\sigma}(\tau) \dot{\sigma}(\tau)^\top d\tau \leq \alpha_2 \|\sigma(0)\|^2 I. \quad (\text{III.4})$$

- (v) For every $\theta \in \mathbb{R}^n$, and every $t \in \mathbb{R}^+$, there exists $t_1(t, \theta) \in [t, t+T_1]$, dependent on θ and t , such that $\theta^\top \dot{\sigma}(t_1(t, \theta)) = 0$.

We remark that [7] provides an $A(t)$ satisfying (i)–(iv) in Assumption 3.2 for $n \in \{2, 3\}$. That this same $A(t)$ also satisfies (v) is shown in Section V. Additionally, using (ii) of this assumption, [7] shows that σ has an additional important property:

Lemma 3.1: Consider (III.2) with $A(t)$ skew-symmetric. Then for all $t \geq 0$, $\|\sigma(t)\| = \|\sigma(0)\|$.

Having $A(t)$ bounded by Assumption 3.2 (i), Lemma 3.1 straightforwardly leads to the following corollary:

Corollary 3.1: Consider (III.2) with $A(t)$ satisfying Assumption 3.2. Then there exists a finite number $\bar{\sigma}'$ such that for all $t \geq 0$, $\|\dot{\sigma}(t)\| \leq \bar{\sigma}'$.

The following assumption on the design constant β in III.1 is further imposed for stability consideration that later appear in Section IV:

Assumption 3.3: The design constant β in III.1 satisfies $\beta > \bar{\sigma}'$.

We conclude this section by motivating (III.1) and (III.2), and contrasting them to the corresponding step in the algorithm of [7]. First observe from [6] that (II.5), (II.6), (II.8) would achieve exponential localization, i.e. drive \hat{x} to x , if \dot{y} were p.e.. The objective in [7] is to force y to asymptotically circumnavigate x at a specified *nonzero* distance from x , on a trajectory on which \dot{y} is p.e.. The capturing or docking objective of Problem 1.1, on the other hand, is fundamentally incompatible with \dot{y} being p.e., as ultimately \dot{y} must approach zero and therefore cannot be p.e.. It is however compatible with the more relaxed requirement that “the degree of

excitation”, to coin a phrase, of \dot{y} be large when y is far from x , and decline as y approaches x .

With this as background, we observe that the first two terms in the right hand side of (III.1), viewed in isolation from the third term, have the role of driving y to the estimated location \hat{x} in a straight line. Should \hat{x} converge to x then of course the convergence of y to \hat{x} will ensure the convergence of y to x , accomplishing the control objective. What the third term in (III.1) does is to ensure that \dot{y} is a signal with a degree of excitation that declines with D . In other words when the docking objective is far from being met, \dot{y} has a large degree of excitation. On the other hand as the docking objective is approached, the degree of excitation declines correspondingly. Such a notion of an *objective driven excitation* to our knowledge is novel. Demonstrating its efficacy in assuring uniform asymptotic convergence, is a key contribution of this paper.

IV. STABILITY AND CONVERGENCE ANALYSIS

This section shows that the closed loop systems defined in (II.2), (II.5)–(III.2), globally, uniformly asymptotically achieves the control objective of problem 1.1. In our analysis, instead of working with the original state vector $[\zeta_1, \zeta_2^\top, y^\top, \hat{x}^\top, \sigma^\top]^\top$, governed by (II.2), (II.5)–(III.2) we work with the state vector

$$\mathcal{X} = [\phi^\top, y^\top, \tilde{x}^\top, p, \sigma^\top]^\top, \quad (\text{IV.1})$$

governed by (II.2), (II.10)–(II.12), (II.14), (III.1), (III.2).

Observe that all elements of the original state space are bounded if this state vector is bounded. Further, the system governing this state space, and indeed the original, constitutes a *nonlinear periodic system*. Moreover, the essential impact of the variables ζ_i is captured by the introduction of ϕ , which is identical to ζ_2 , and p , which captures important aspects of the error dynamics. Finally the global objective, i.e. that y should converge to x , is also demonstrated by working with \mathcal{X} . Noting, thus, that it suffices to work with this self contained new state space and its governing dynamics, Section IV-A proves the boundedness of all signals appearing in the closed loop, and Section IV-B proves global uniform asymptotic convergence.

A. Boundedness

As flagged above we will now prove that \mathcal{X} defined in (IV.1) is bounded. To this end we need the following Lemma.

Lemma 4.1: Consider $\rho : \mathbb{R} \rightarrow \mathbb{R}^n$ that obeys:

$$\dot{\rho}(t) = -(\bar{\alpha} - g(t))\rho(t) + \rho_0(t),$$

where $\bar{\alpha} > 0$, $\rho_0 : \mathbb{R} \rightarrow \mathbb{R}^n$ is bounded and $g : \mathbb{R} \rightarrow \mathbb{R}$ is in \mathcal{L}_2 . Then $\rho(\cdot)$ is bounded.

Proof: See [1]. ■

Next we show the boundedness of closed loop signals.

Theorem 4.1: Consider (II.2), (II.10)–(II.12), (II.14), (III.1), (III.2), with Assumptions 3.1 and 3.2 in force. Then \mathcal{X} in (IV.1) is bounded.

Proof: See [1]. ■

B. Uniform Asymptotic Convergence

Next, the main result of convergence is presented.

Theorem 4.2: Consider (II.2), (II.10)–(II.12), (II.14), (III.1), (III.2), with Assumptions 3.1–3.3 in force and let $\sigma(0) \neq 0$. Then the following converges uniformly asymptotically to zero:

$$[\tilde{x}^\top(t), y^\top(t) - \hat{x}^\top(t), \phi^\top(t), p(t)]^\top.$$

Proof: See [1]. ■

V. SELECTION OF $A(t)$

Reference [7] presents a procedure for the selection of $A(t)$ that assures (i)–(iv) of Assumption 3.2 for $n \in \{2, 3\}$. In this section we show that this same choice also satisfies (v) of Assumption 3.2 for $n \in \{2, 3\}$.

Consider first $n = 2$: With

$$E = \begin{bmatrix} 0 & 1 \\ -1 & 0 \end{bmatrix}, \quad (\text{V.1})$$

the matrix

$$A(t) = aE, \quad a \in \{\mathbb{R} \setminus \{0\}\}, \quad (\text{V.2})$$

has been shown in [7] to satisfy (i)–(iv) of Assumption 3.2 with

$$T_1 = \frac{\pi}{|a|}. \quad (\text{V.3})$$

We now show that (V.2) satisfies (v) of Assumption 3.2 as well.

Theorem 5.1: With $\sigma : \mathbb{R} \rightarrow \mathbb{R}^2$ consider (III.2), with $A : \mathbb{R} \rightarrow \mathbb{R}^{2 \times 2}$ as in (V.1) and (V.2). Then σ obeys (v) of Assumption 3.2 with T_1 as in (V.3).

Proof: See [1]. ■

For $n = 3$ the matrix $A(t)$ is defined in [7] as below. Effectively, $A(t)$ in this case switches periodically between the two 3×3 matrices

$$B = \begin{bmatrix} 0 & 0 \\ 0 & bE \end{bmatrix}, \quad \text{and} \quad (\text{V.4})$$

$$C = \begin{bmatrix} cE & 0 \\ 0 & 0 \end{bmatrix} \quad (\text{V.5})$$

b and c being real nonzero scalars. To ensure that the resulting matrix is differentiable, we require a differentiable transition between B and C . To achieve this [7] defines a nondecreasing $g : \mathbb{R} \rightarrow \mathbb{R}$, that obeys:

$$g(t) = 0 \quad \forall t \leq 0 \quad (\text{V.6})$$

$$g(t) = 1, \quad \forall t \geq 1, \quad \text{and} \quad (\text{V.7})$$

$$g(t) \text{ is twice differentiable } \forall t. \quad (\text{V.8})$$

An example of such a $g(t)$ is

$$g(t) = \begin{cases} \frac{1}{2}(1 - \cos(\pi t)) & 0 \leq t \leq 1 \\ 0 & t < 0 \\ 1 & t > 1. \end{cases} \quad (\text{V.9})$$

Clearly, (V.9) satisfies (V.6) and (V.7). Further (V.8) holds since

$$\lim_{t \rightarrow 0^+} \dot{g}(t) = \lim_{t \rightarrow 1^-} \dot{g}(t) = 0.$$

Now, for nonzero scalars b and c , we select $A(t)$ as follows. For a suitably small $\rho > 0$, define

$$\bar{T}_1 = \rho, \quad \bar{T}_2 = \rho + \frac{\pi}{|b|}, \quad \bar{T}_3 = 2\rho + \frac{\pi}{|b|}, \quad (\text{V.10})$$

and

$$\bar{T}_4 = 3\rho + \frac{\pi}{|b|}, \quad \bar{T}_5 = 3\rho + \frac{\pi}{|b|} + \frac{\pi}{|c|}, \quad T_1 = \bar{T}_6 = 4\rho + \frac{\pi}{|b|} + \frac{\pi}{|c|}. \quad (\text{V.11})$$

For all t , let $K_{T_1}(t)$ denote the largest integer k satisfying $t \geq kT_1$ and let $r_{T_1}(t) = t - K_{T_1}(t)T_1$. Then [7] defines $A(t)$ as

$$A(t) = \begin{cases} g\left(\frac{r_{T_1}(t)}{\rho}\right) B & 0 \leq r_{T_1}(t) \leq \bar{T}_1 \\ B & \bar{T}_1 \leq r_{T_1}(t) \leq \bar{T}_2 \\ \left(1 - g\left(\frac{r_{T_1}(t) - \bar{T}_2}{\rho}\right)\right) B & \bar{T}_2 \leq r_{T_1}(t) \leq \bar{T}_3 \\ g\left(\frac{r_{T_1}(t) - \bar{T}_3}{\rho}\right) C & \bar{T}_3 \leq r_{T_1}(t) \leq \bar{T}_4 \\ C & \bar{T}_4 \leq r_{T_1}(t) \leq \bar{T}_5 \\ \left(1 - g\left(\frac{r_{T_1}(t) - \bar{T}_5}{\rho}\right)\right) C & \bar{T}_5 \leq r_{T_1}(t) \leq \bar{T}_6 \end{cases} \quad (\text{V.12})$$

Then we have the following theorem:

Theorem 5.2: Consider (III.2) with $A(t)$ and T_1 , defined in (V.10)–(V.12). Then for every pair of nonzero b, c , (v) of Assumption 3.2 holds.

Proof: See [1]. ■

VI. SIMULATIONS

In this section, we provide the results of a set of simulation examples in \mathbb{R}^3 in order to demonstrate the performance of the adaptive localization and motion control scheme (II.2), (II.5), (II.6), (II.8), (III.1), (III.2), (V.4), (V.5), (V.9), (V.10)–(V.12). For comparison purposes, we consider the target settings in the examples of [6]. In all the examples, the design parameters and functions are selected as follows: $\alpha = 1$, $\gamma = 10$, $f(D) = 1 - e^{-D}$, $\beta = 3$, $b = c = 1$, $\rho = 0.1$ and $\sigma(0) = [0.6, 0.6, 0.6]^\top$.

Example 1: The target is stationary located at $x = [2, 3, 2]^\top$ (m). Using the adaptive scheme, we obtain the results shown in Figure 1. As can be seen in Figure 1, the agent successfully converges to the target location.

Example 2: This example is intended to test the robustness of the adaptive scheme to slow but persistent drifts in the target location. The target is moving around a nominal location at $x_n = [2, 3, 2]^\top$ (m) and its trajectory is given by $x(t) = [2 + \sin 0.005t, 3 + \cos 0.005t, 2]^\top$ (m). Observe that the net extent of the drift in the first two coordinates is 2, and thus substantial. The rate of drift (\dot{x}) on the other hand is relatively small having an amplitude of 0.005.

For this example, using the adaptive scheme, we obtain the results shown in Figure 2, while Figure 3 provides a snapshot of the initial tracking. $y(t)$ tracks the motion of $x(t)$ with a small error.

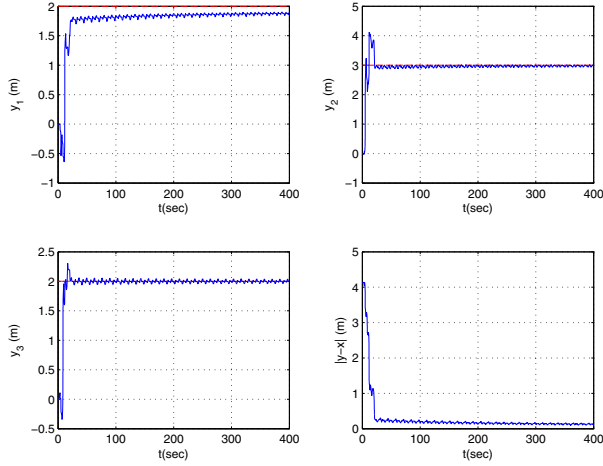


Fig. 1. Agent motion for Example 1. The dashed lines correspond to the actual coordinates of the target T and the solid curves show the trajectories of the mobile agent A .

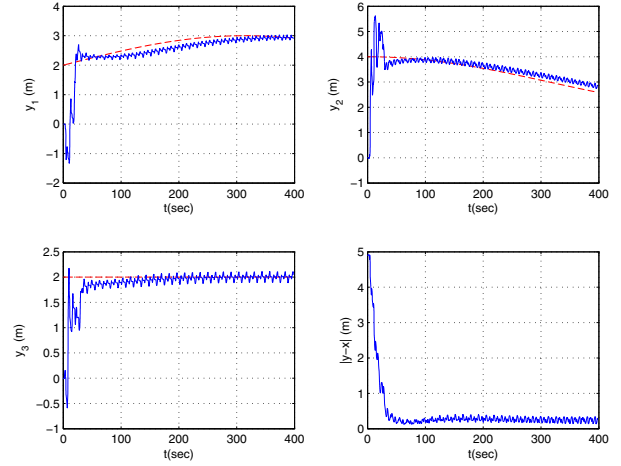


Fig. 3. Agent motion for Example 2 for $t \in [0, 400]$ (sec). The dashed lines correspond to the actual coordinates of the target T and the solid curves show the trajectories of the mobile agent A .

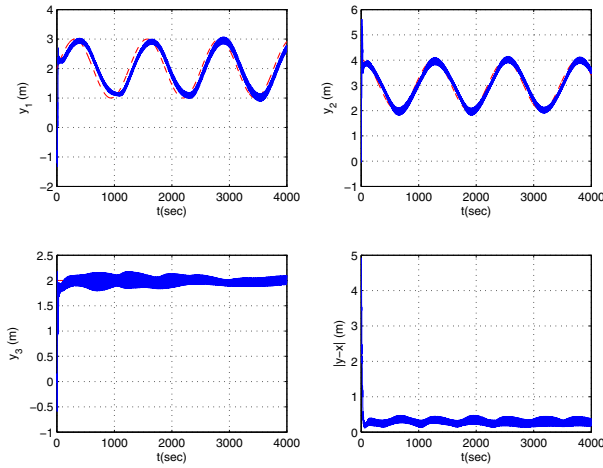


Fig. 2. Agent motion for Example 2 for $t \in [0, 4000]$ (sec). The dashed lines correspond to the actual coordinates of the target T and the solid curves show the trajectories of the mobile agent A .

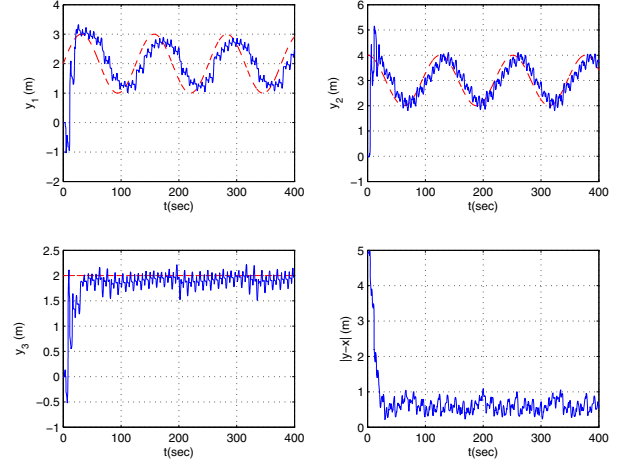


Fig. 4. Agent motion for Example 3. The dashed lines correspond to the actual coordinates of the target T and the solid curves show the trajectories of the mobile agent A .

Example 3: This example is similar to Example 2, but the target drift rate is ten times that of Example 2, i.e. $x(t) = [2 + \sin 0.05t, 3 + \cos 0.05t, 2]^T$ (m). Figure 4 shows the tracking behavior. As expected the tracking though still quite good is with correspondingly larger error.

Example 4: Similar to Example 1, the target is stationary located at $x = [2, 3, 2]^T$ (m). In this example, we test noise performance, assuming that the distance measurement $D(t)$ is perturbed by a zero mean bandlimited white Gaussian noise. Figures 5 and 6, respectively, show the results with noise variances 0.01 (m^2) and 0.05 (m^2). (We would like to note that there is typo in the results shown in Figures 5,6,8 of [6]; the noises variances for these figures ought to be 0.01 , 0.05 , 0.01 , respectively, instead of 0.001 , 0.005 , 0.001 .) As can be seen in these figures, the agent successfully converges to the close vicinity of the target. As expected, the tracking error scales with the standard deviation of the noise.

Example 5: Similar to Example 3, the target is moving around a nominal location at $x_n = [2, 3, 2]^T$ (m) and its trajectory is given by $x(t) = [2 + \sin 0.05t, 3 + \cos 0.05t, 2]^T$ (m). For this drifting target case, we test noise performance, assuming that the distance measurement $D(t)$ is perturbed by a zero mean bandlimited white Gaussian noise with noise variance 0.01 (m^2). Figure 7 shows the results. As can be seen in Figure 1, the agent successfully converges to the close vicinity of the mobile target. The additional tracking error magnitude compared to Example 2 is of the magnitude of the measurement noise.

VII. CONCLUSION

We have presented an adaptive scheme for localization of a target from distance measurements and motion control of a mobile agent to track and capture this target. The adaptive scheme is composed of a robust adaptive law that

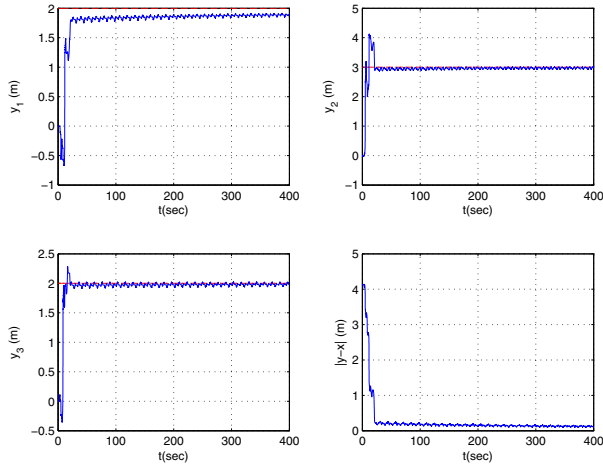


Fig. 5. Agent motion for Example 4 with noise variance equal to $0.01 \text{ (m}^2\text{)}$. The dashed lines correspond to the actual coordinates of the target T and the solid curves show the trajectories of the mobile agent A .

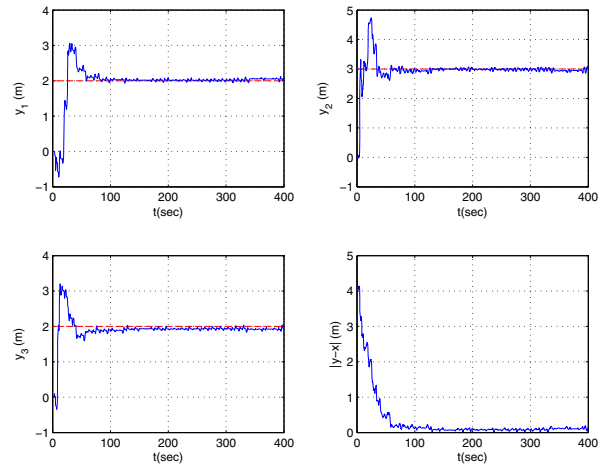


Fig. 6. Agent motion for Example 4 with noise variance equal to $0.05 \text{ (m}^2\text{)}$. The dashed lines correspond to the actual coordinates of the target T and the solid curves show the trajectories of the mobile agent A .

generates a location estimate of the target using distance measurements, and a motion control law that moves the mobile agent towards the estimated location. A stability analysis for the overall adaptive control scheme is presented. The results are valid in both two and three dimensions of motion space. Simulation results are provided as well, demonstrating the performance of the proposed adaptive localization and motion control scheme as well as robustness of the scheme against slow bounded drifts in positions of the target and distance measurement noise.

As a follow-up study the authors are currently working on extension of the design for cooperative target pursuit by a formation of autonomous agents. A further research direction is investigation of single agent and cooperative target pursuit problems, defined similarly to this paper, but using bearing measurements instead of range measurements, noting that a set of related techniques were developed in [16].

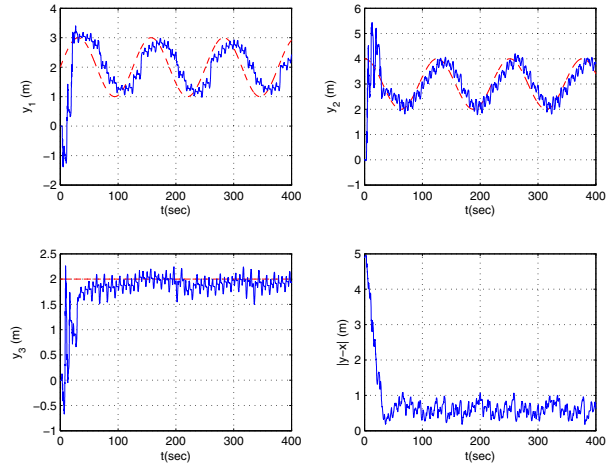


Fig. 7. Agent motion for Example 5. The dashed lines correspond to the actual coordinates of the target T and the solid curves show the trajectories of the mobile agent A .

REFERENCES

- [1] B. Fidan, S. Dasgupta, and B. Anderson, "Adaptive range-measurement-based target pursuit," accepted to appear in *Int. Journal of Adaptive Control and Signal Processing*.
- [2] A. Bishop, B. Fidan, B. Anderson, K. Doğançay, and P. Pathirana, "Optimality analysis of sensor-target localization geometries," *Automatica*, vol. 46, no. 3, pp. 479–492, March 2010.
- [3] S. Martinez and F. Bullo, "Optimal sensor placement and motion coordination for target tracking," *Automatica*, vol. 42, no. 4, pp. 661–668, March 2006.
- [4] *IEEE Signal Processing Magazine*, July 2005.
- [5] G. Mao and B. Fidan (editors), *Localization Algorithms and Strategies for Wireless Sensor Networks*, IGI Global - Information Science Publishing, 2009.
- [6] S. Dandach, B. Fidan, S. Dasgupta, and B. Anderson, "A Continuous Time Linear Adaptive Source Localization Algorithm Robust to Persistent Drift," *Systems and Control Letters*, vol. 58, pp. 7–16, 2009.
- [7] I. Shames, S. Dasgupta, B. Fidan, and B. Anderson, "Circumnavigation from distance measurements under slow drift," *IEEE Tr. on Automatic Control*, vol. 57, no. 4, pp. 889–903, April 2012.
- [8] I. Shames, B. Fidan, and B. Anderson, "Close target reconnaissance with guaranteed collision avoidance," *Int. J. Robust and Nonlinear Control*, vol. 21, no. 16, pp.1823–1840, 2011.
- [9] S. Bopardikar, F. Bullo, and J. Hespanha, "On discrete-time pursuit-evasion games with sensing limitations," *IEEE Tr. on Robotics*, vol.24, no.6, pp.1429–1439, December 2008.
- [10] T.-H. Kim and T. Sugie, "Cooperative control for target-capturing task based on a cyclic pursuit strategy," *Automatica*, vol. 43, pp. 1426–1431, 2007.
- [11] A. Bishop, B. Fidan, B. Anderson, K. Doğançay, and P. Pathirana, "Optimal range-difference based localization considering geometrical constraints," *IEEE Journal of Oceanic Engineering*, vol. 33, no. 3, pp. 289–301, July 2008.
- [12] A. Bishop, B. Fidan, K. Doğançay, B. Anderson, and P. Pathirana, "Exploiting geometry for improved hybrid AOA/TDOA based localization," *Signal Processing*, vol. 88, no. 7, pp. 1775–1791, July 2008.
- [13] P. Ioannou and B. Fidan, *Adaptive Control Tutorial*, Prentice-Hall, 2006.
- [14] P. Ioannou and J. Sun, *Robust Adaptive Control*, Prentice-Hall, 1996.
- [15] B. Anderson, "Exponential stability of linear equations arising in adaptive identification," *IEEE Transactions on Automatic Control*, pp. 530–538, May–June 1977.
- [16] M. Deghat, I. Shames, B. Anderson, and C. Yu. "Target localization and circumnavigation using bearing measurements in 2D," in *Proc. IEEE Conference on Decision and Control*, pp. 334–339, December 2010.